Robotica (2015) volume 33, pp. 828–847. © Cambridge University Press 2014
doi:10.1017/S0263574714000526

Modal space decoupled optimal design for a class of symmetric spatial parallel mechanisms with consideration of passive joint damping

Tian Ti-Xian, Jiang Hong-Zhou*, Tong Zhi-Zhong and He Jing-Feng

School of Mechatronics Engineering, Harbin Institute of Technology, Harbin, 150001, P.R. China

(Accepted February 8, 2014. First published online: March 17, 2014)

SUMMARY

In this study, we analyze the influence of passive joint viscous friction (PJVF) on modal space decoupling for a class of symmetric spatial parallel mechanisms (SSPM). The Jacobian matrix relating the platform movements to each passive joint velocity is first gained by vector analysis and the passive joint damping matrix is then derived by applying the Kane method. Next, an analytic formula index measuring the degree of coupling effects between the damping terms in the modal coordinates is proposed using classical modal analysis of dynamic equations in task space. Based on the index, a new optimal design method is found which establishes the kinematics parameters for minimizing the coupling degree of damping and achieves optimal fault tolerance for modal space decoupling when all struts have identical damping and stiffness coefficients in their axial directions. To illustrate the effectiveness of the theory, the new method was used to redesign two configurations of a specific manipulator.

KEYWORDS: Passive joints; Kane method; Coupling; Optimal design method; Modal space decoupling.

Nomenclature

$\mathbf{a}_i$	the vector of the upper joint point
$\mathbf{b}_i$	the vector of the lower joint point
r_a	distribution radius of upper joint points
r_b	distribution radius of lower joint points
α	the half central angle for the upper joints
β	the half central angle for the lower joints
H	the height between the upper and lower joint plane
h	the height of the payload center
$\mathbf{M}_t$	inertia matrix in task space
$\mathbf{B}_t$	damping matrix in task space
$\mathbf{K}_t$	stiffness matrix in task space
$\mathbf{J}_{lx}$	Jacobian matrix
$\mathbf{l}$	the length vector of the actuator
$\mathbf{x}$	the vector of the platform position
$\mathbf{q}$	the modal coordinate
δ	the index based on the modal damping matrix
$\mathbf{U}$	the modal matrix
Ω	the modal frequency matrix
$\mathbf{D}$	the modal damping matrix

* Corresponding author. E-mail: jianghz@hit.edu.cn

f	the generalized damping forces of the system
f^*	the generalized active forces of the system
T_{pj}	the friction torque of the passive joint j
B_{pj}	the damping coefficient of the passive joint j
ω_{pj}	the angular velocity of the passive joint j
$\mathbf{J}_{pj,x}$	Jacobian matrix relating the j passive joint velocity to platform velocity
B_{cri}, B_{cdi1}, B_{cdi1}, B_{cdi2}, B_{cui1}, B_{cui2}	the damping coefficients of the related passive joints, respectively
$\mathbf{J}_{r,i}$, $\mathbf{J}_{di1,x}$,$\mathbf{J}_{di2,x,}$ $\mathbf{J}_{ui1,x,}$ $\mathbf{J}_{ui2,x}$	the Jacobian matrix relating the related passive joint velocity to platform velocity, respectively
$\mathbf{l}_{n,1}$	the unitary direction vector of the first leg
$\mathbf{v}_1$	the vector representing $\mathbf{l}_{n,1} \times \mathbf{a}_1$
m	the mass of the payload
I_{xx}, I_{yy}, I_{zz}	the moments of inertia of the payload
$\mathbf{M}_d$	modal mass matrix
$D_\perp$	the coupling term of the modal damping matrix $\mathbf{D}$
D_o	the proportional damping term of the modal damping matrix $\mathbf{D}$
θ	damping coupling angle
n	radius ratio
w_1, w_2, w_3, w_4, w_5	weighting factors
$\mathbf{C}_{cd1}$, $\mathbf{C}_{cd2,}$ $\mathbf{C}_{cu1}$, $\mathbf{C}_{cu2}$, $\mathbf{C}_{cr}$	the normalized damping matrices of the related passive joints, respectively

1. Introduction

In the past few decades, parallel mechanisms have attracted a great deal of attention, and this technology has seen a variety of applications, such as in motion simulators, micro positioning devices, and vibration isolation platforms. This focus on parallel mechanisms is primarily driven by their high load/mass ratio capability and the potential for high precision.[1,2,3] However, the system couplings resulting from the complex dynamic characteristics of such parallel manipulators may degrade the control performance (lower system precision and have undesired cross-coupling outputs), which means changing one input to control its corresponding output will affect other outputs.

In the literature, pioneering attempts[4,5] have been undertaken to decouple multiple-input multiple-output (MIMO) plants into single-input single-output (SISO) plants. McInroy[4] proposed two decoupling algorithms by combining static input–output transformations with hexapod geometric design. Chen and McInroy,[5] then proposed a modal space decoupled controller which maps input–output variables from the joint space to the decoupled modal space using singular value decomposition of the joint space inverse mass matrix. McInroy[6] proposed a design method to get the dynamically decoupled and equalized manipulator. Plummer,[7,8,9,10] presented a modal position controller for improving the performance of an electro-hydrostatic flight simulator motion system. In all these cases, the system is simplified as a proportional damping system where passive joint viscous friction (PJVF) is simply ignored, because of the size and motion amplitudes of the passive joints. However, not every parallel mechanism necessarily has small and frictionless passive joints. Thus, a PJVF system becomes a damping coupling system.

It is clear that systems with damping coupling can be decoupled within the framework of state-variable models,[11,12,13] but these models lack the transparency of the usual second-order models, and hence, have not found their way into daily engineering practice.

Engineers feel more comfortable when working with proportional damped systems. However, to the best of our knowledge, no one has yet built a PJVF model and determined the relationship between the degree of coupling effects caused by PJVF and the kinematics parameters for symmetric spatial parallel mechanisms (SSPM) considered in this study, which will lead to an optimal design method.

https://doi.org/10.1017/S0263574714000526 Published online by Cambridge University Press

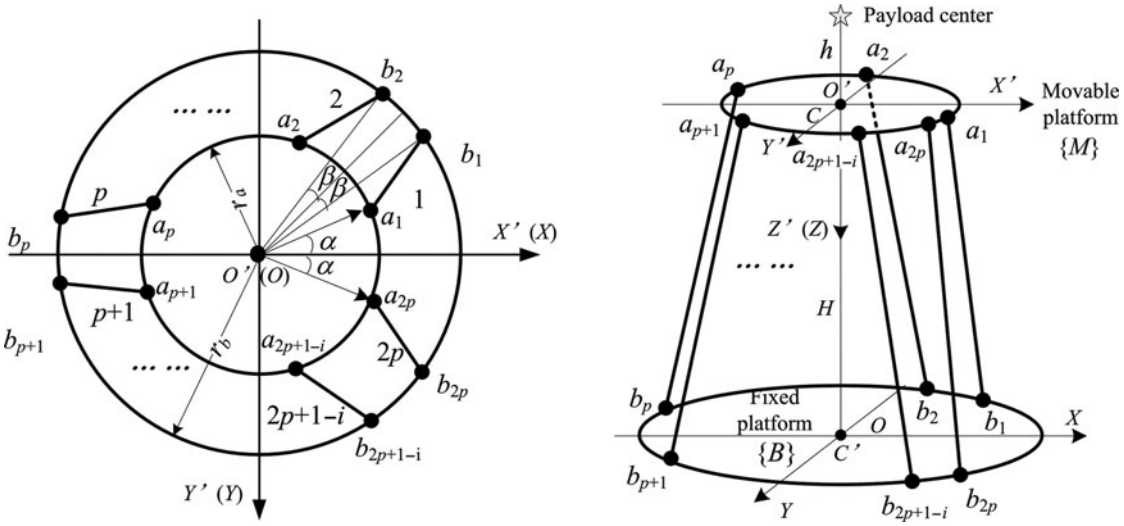

Fig. 1. Schematic of a symmetric spatial parallel mechanism (SSPM) with $2p$ struts.

In this paper, we propose a new optimal design method to reduce the coupling between modal coordinates due to joint damping and achieve optimal fault tolerance for modal space decoupling by choosing the geometry of parallel mechanisms.

This paper is organized as follows. Section 2 presents a concise survey on the theory of modal decoupling. This survey sets up the terminology and notation used throughout the paper. In Section 3, the explicit dynamic modal including PJVF and an analytical formulation of a modal matrix in task space for the SSPM is derived. An index measuring the degree of coupling effects between the damping terms in the modal coordinates is expressed in analytical form as functions of the configuration parameters. In Section 4, the relationship between the degree of coupling effects caused by each part of the PJVF and geometry configuration parameters, is explored. In Section 5, the optimal conditions, including optimal function and optimization constraints, are discussed and an optimal design method is proposed for determining the geometry configuration parameters using an iterative procedure. Finally, we present our conclusions.

2. Problem Formulation

Figure 1 shows a class of symmetric parallel mechanisms with $N = 2p$ ($p \in Z$, Z is the set of positive integers, and $p \geq 3$) actuators under study. In this manipulator, the spatial motion of the moving platform is generated by $2p$ piston–cylinder actuators. Each piston–cylinder actuator consists of two parts connected by a universal joint. The actuators are connected to the fixed base and the moving platform by universal joints at points $\mathbf{a}_i$ and $\mathbf{b}_i$, where $i = 1 \ldots 2p$. The upper and lower joint points $\mathbf{a}_i$ and $\mathbf{b}_i$ are located on circles with radii of r_a and r_b (C and C' are the centers of these two circles). Figure 1 shows the inertial coordinates $\{\mathrm{B}\}$: O-XYZ in the base and fixed coordinates $\{\mathrm{M}\}$: O′-X′Y′Z′ in the moving platform. α and β denote the half central angle for the upper and lower joints. The height between the upper and lower joint plane is H. The height of the payload center is h.

In this paper, the proportional viscous friction in the passive joints is considered, then the vibration equation in the task space for the SSPM is:

$$\mathbf{M}_t\ddot{\mathbf{x}} + \mathbf{B}_t\dot{\mathbf{x}} + \mathbf{K}_t\mathbf{x} = \mathbf{0}, \tag{1}$$

where $\mathbf{M}_t$ is a 6×6 inertia matrix in task space, $\mathbf{B}_t$ is a 6×6 damping coefficient matrix caused by PJVF, $\mathbf{K}_t = \mathbf{J}_{lx}^{\mathrm{T}}\mathbf{K}_l\mathbf{J}_{lx}$, $\mathbf{J}_{lx}$ is a $2p\times 6$ Jacobian matrix relating the platform velocities to the actuator length rates in the joint space, $\mathbf{J}_{lx}\dot{\mathbf{x}} = \dot{\mathbf{l}}.\mathbf{K}_l = \mathrm{diag}(k_{li})$, k_{li} is the stiffness coefficient of the ith leg, and $i = 1\ldots 2p$.

https://doi.org/10.1017/S0263574714000526 Published online by Cambridge University Press

The differential matrix Eq. (1) is highly coupled. The ith component equation involves not only $\mathbf{x}_i$ and its derivatives but also other coordinates and their derivatives.

Now let $\mathbf{U}$ be a modal matrix that satisfies:

$$\mathbf{x} = \mathbf{U}\mathbf{q}. \tag{2}$$

In terms of the principal coordinate $\mathbf{q}$, the equation for damped free vibration takes the canonical form:

$$\ddot{\mathbf{q}} + \mathbf{D}\dot{\mathbf{q}} + \mathbf{\Omega}^2\mathbf{q} = \mathbf{0}, \tag{3}$$

where $\mathbf{\Omega} = \sqrt{\mathbf{U}^{\mathrm{T}}(\mathbf{M}_t^{-1}\mathbf{K}_t)\mathbf{U}}$ is the modal frequency matrix and $\mathbf{D} = \mathbf{U}^{\mathrm{T}}(\mathbf{M}_t^{-1}\mathbf{B}_t)\mathbf{U}$ is the modal damping matrix.

A system has proportional damping if it can be decoupled by a real modal matrix $\mathbf{U}$, whereby the modal damping matrix $\mathbf{D}$ is diagonal. A system is proportionally damped if $\mathbf{B}_t = \alpha\mathbf{M}_t + \beta\mathbf{K}_t$, where α and β are constants. However, because of passive viscous friction, there is no reason the condition should be satisfied.

Over the years, various types of decoupling approximations were employed in the analysis of damped systems.[20–22] Several indices for the quantification of damping coupling were also proposed in.[23–26] These indices can be classified into two types: one based on individual complex modes and one based on the modal damping matrix or mass-normalized damping matrix. The indices based on the modal damping matrix are of analytical value if the modal damping matrix is known.

The index proposed in[26] is defined as:

$$\delta = \sum_{i=1}^{6}\sum_{j=1,j\neq i}^{6}\left|\mathbf{D}_{ij}\right| \Bigg/ \sum_{i=1}^{6}\sum_{j=1}^{6}\left|\mathbf{D}_{ij}\right|. \tag{4}$$

If $\delta = 0$, damping is proportional and if $\delta \ll 1$, the system can be considered as a proportional damping system.

To design so that $\mathbf{D}$ is a diagonal approximation, parameters must be chosen to ensure the index δ is small enough, and we need to find an optimal configuration as close to the ideal proportional damped configuration as possible with simultaneously fewer coupling effects in modal space.

3. Classical Modal Analysis

In this section, a classical modal analysis is used to obtain an analytic formula index which measures the degree of coupling effects of the modal damping matrix $\mathbf{D}$.

3.1. Passive joints viscous friction modeling for SSPM

In the literature, closed form dynamic equations for SSPM assuming rigid legs, a stationary base and frictionless passive joints were derived using the Newton–Euler,[14,15] Lagrange,[16,17] or Kane methods.[18,19] However, to characterize the PJVF influence, the model for the SSPM including PJVF must first be established.

Viscous friction forces have a simple equation:

$$T_{pj} = B_{pj}\omega_{pj}, \tag{5}$$

where T_{pj} is the friction torque of the passive joint j, and B_{pj} and ω_{pj} are the corresponding damping coefficient and angular velocity respectively.

To calculate the viscous friction force in the passive joint j, it is necessary to determine the angular velocity. Its explicit formulation is derived in Appendix A by vector analysis of the kinematics.Explicit PJVF formulation is derived using the Kane method. The Kane method is a projection method, this method in which all active forces and damping forces are projected along a limited set of generalized velocities, will be central in the derivation of the motion system mechanical model. Considering only

https://doi.org/10.1017/S0263574714000526 Published online by Cambridge University Press

PJVF of SSPM, the Kane equation can be expressed as:

$$f + f^* = 0, \tag{6}$$

where f and f^* are the generalized damping forces and active forces of the system.

Choosing the platform velocity $\dot{\mathbf{x}}$ as the generalized velocity for the system, the generalized damping forces of a SSPM can be projected along the generalized velocity by:

$$f = \sum_{j=1}^{N} J_{pj,x}^{\mathrm{T}} T_{pj}, \tag{7}$$

where $J_{pj,x}$ is a Jacobian matrix relating the passive joint velocity to platform velocity.

Combining Eqs. (5) and (6), gives Eq. (7) written as:

$$f = \sum_{i=1}^{2p} \left(B_{cri}\mathbf{J}_{r,i}^{\mathrm{T}}\mathbf{J}_{r,i} + B_{cdi1}\mathbf{J}_{di1,x}^{\mathrm{T}}\mathbf{J}_{di1,x} + B_{cdi2}\mathbf{J}_{di2,x}^{\mathrm{T}}\mathbf{J}_{di2,x} + B_{cui1}\mathbf{J}_{ui1,x}^{\mathrm{T}}\mathbf{J}_{ui1,x} + B_{cui2}\mathbf{J}_{ui2,x}^{\mathrm{T}}\mathbf{J}_{ui2,x} \right)\dot{\mathbf{x}}, \tag{8}$$

where B_{cri}, B_{cdi1}, B_{cdi2}, B_{cui1}, and B_{cui2} reflect the damping coefficients of the ith passive joints.

The generalized active forces for the system can be expressed as:

$$f^* = \mathbf{B}_t\dot{\mathbf{x}}. \tag{9}$$

Inserting Eqs. (8) and (9) into the Kane Eq. (6) gives the explicit passive joint damping matrix in task space derived as:

$$\mathbf{B}_t = \sum_{i=1}^{2p} \left(B_{cri}\mathbf{J}_{r,i}^{\mathrm{T}}\mathbf{J}_{r,i} + B_{cdi1}\mathbf{J}_{di1,x}^{\mathrm{T}}\mathbf{J}_{di1,x} + B_{cdi2}\mathbf{J}_{di2,x}^{\mathrm{T}}\mathbf{J}_{di2,x} + B_{cui1}\mathbf{J}_{ui1,x}^{\mathrm{T}}\mathbf{J}_{ui1,x} + B_{cui2}\mathbf{J}_{ui2,x}^{\mathrm{T}}\mathbf{J}_{ui2,x} \right). \tag{10}$$

If the passive joints are assumed to have identical damping coefficients in each axial direction, a concise expression for $\mathbf{B}_t$ is obtained, which is derived in Appendix B:

$$\mathbf{B}_t = \begin{bmatrix} \mathrm{diag}([B_{tx} \quad B_{ty} \quad B_{tz}]^{\mathrm{T}}) & \tilde{\boldsymbol{\rho}}_t \\ -\tilde{\boldsymbol{\rho}}_t & \mathrm{diag}([B_{txx} \quad B_{tyy} \quad B_{tzz}]^{\mathrm{T}}) \end{bmatrix}. \tag{11}$$

where $\tilde{\boldsymbol{\rho}}_t = \begin{bmatrix} 0 & -\rho_{tz} & 0 \\ \rho_{tz} & 0 & 0 \\ 0 & 0 & 0 \end{bmatrix}$.

3.2. Classical Modal decoupling

Modal matrix $\boldsymbol{U}$ and frequency matrix $\boldsymbol{\Omega}$ can be obtained by solving the Eigen problem:

$$\mathbf{K}_t\mathbf{u} = \lambda\mathbf{M}_t\mathbf{u}. \tag{12}$$

The undamped Eigen problem, Eq. (12), has been solved by Jiang *et al.*[27] in joint space, and HE Jing-feng *et al.*[28] in task space, when it was supposed that the platform is at a neutral pose, the inertial effects of all the actuators are not considered, the origins O′(O) of the coordinate systems are placed at the center of gravity (COG) of the payload and the $2p$ actuators have identical stiffness, i.e., $k_{li} = k$.

Using their results, the frequency matrix $\boldsymbol{\Omega}$ can be obtained when using the unitary direction vector $\mathbf{l}_{n,1} = [\mathbf{l}_{n1x} \quad \mathbf{l}_{n1y} \quad \mathbf{l}_{n1z}]^{\mathrm{T}}$ and the vector $\mathbf{v}_1 = [\mathrm{v}_{1x} \quad \mathrm{v}_{1y} \quad \mathrm{v}_{1z}]^{\mathrm{T}}$ of the first leg:

$$\boldsymbol{\Omega} = \sqrt{k \cdot \mathbf{M}_d^{-1}}, \tag{13}$$

https://doi.org/10.1017/S0263574714000526 Published online by Cambridge University Press

where $\mathbf{M}_d^{-1} = \mathrm{diag}([\,\lambda_1 \quad \lambda_2 \quad \lambda_3 \quad \lambda_4 \quad \lambda_5 \quad \lambda_6\,])$,

$$\lambda_1 = \frac{2p\mathbf{v}_{n1z}^2}{I_{zz}}$$

$$\lambda_2 = \frac{p}{2m}\left(\frac{m}{I_{xx}}\left(\mathbf{v}_{1x}^2+\mathbf{v}_{1y}^2\right)+\mathbf{l}_{n1y}^2+\mathbf{l}_{n1x}^2-\left(\left(\frac{m}{I_{xx}}\left(\mathbf{v}_{1y}^2-\mathbf{v}_{1x}^2\right)+\mathbf{l}_{n1x}^2-\mathbf{l}_{n1y}^2\right)^2 + 4\left(\frac{m}{I_{xx}}\mathbf{v}_{1y}\mathbf{v}_{1x}-\mathbf{l}_{n1x}\mathbf{l}_{n1y}\right)^2\right)^{\frac{1}{2}}\right)$$

$$\lambda_3 = \frac{p}{2m}\left(\frac{m}{I_{xx}}\left(\mathbf{v}_{1x}^2+\mathbf{v}_{1y}^2\right)+\mathbf{l}_{n1y}^2+\mathbf{l}_{n1x}^2+\left(\left(\frac{m}{I_{xx}}\left(\mathbf{v}_{1y}^2-\mathbf{v}_{1x}^2\right)+\mathbf{l}_{n1x}^2-\mathbf{l}_{n1y}^2\right)^2 + 4\left(\frac{m}{I_{xx}}\mathbf{v}_{1y}\mathbf{v}_{1x}-\mathbf{l}_{n1x}\mathbf{l}_{n1y}\right)^2\right)^{\frac{1}{2}}\right)$$

$$\lambda_4 = \frac{2p\mathbf{l}_{n1z}^2}{m}$$

$$\lambda_5 = \frac{p}{2m}\left(\frac{m}{I_{yy}}\left(\mathbf{v}_{1\mathrm{x}}^2+\mathbf{v}_{1\mathrm{y}}^2\right)+\mathbf{l}_{n1y}^2+\mathbf{l}_{n1x}^2-\left(\left(\frac{m}{I_{yy}}\left(\mathbf{v}_{1y}^2-\mathbf{v}_{1x}^2\right)+\mathbf{l}_{n1x}^2-\mathbf{l}_{n1y}^2\right)^2 + 4\left(\frac{m}{I_{yy}}\mathbf{v}_{1y}\mathbf{v}_{1x}-\mathbf{l}_{n1x}\mathbf{l}_{n1y}\right)^2\right)^{\frac{1}{2}}\right)$$

$$\lambda_6 = \frac{p}{2m}\left(=\frac{m}{I_{yy}}\left(\mathbf{v}_{1\mathrm{x}}^2+\mathbf{v}_{1\mathrm{y}}^2\right)+\mathbf{l}_{n1y}^2+\mathbf{l}_{n1x}^2+\left(\left(\frac{m}{I_{yy}}\left(\mathbf{v}_{1y}^2-\mathbf{v}_{1x}^2\right)+\mathbf{l}_{n1x}^2-\mathbf{l}_{n1y}^2\right)^2 + 4\left(\frac{m}{I_{yy}}\mathbf{v}_{1y}\mathbf{v}_{1x}-\mathbf{l}_{n1x}\mathbf{l}_{n1y}\right)^2\right)^{\frac{1}{2}}\right),$$

m is the mass of the payload, I_{xx}, I_{yy}, I_{zz} are the moments of inertia of the payload, and

$$\mathbf{v}_{1x} = \mathbf{l}_{n1z}\mathrm{a}_{1y} - \mathbf{l}_{n1y}\mathrm{a}_{1z}, \quad \mathbf{v}_{1y} = \mathbf{l}_{n1x}\mathrm{a}_{1z} - \mathbf{l}_{n1z}\mathrm{a}_{1x}, \quad \mathbf{v}_{1z} = \mathbf{l}_{n1y}\mathrm{a}_{1x} - \mathbf{l}_{n1x}\mathrm{a}_{1y}$$

We then find an explicit formula for the modal matrix expressed as:

$$\mathbf{U} = \frac{1}{\sqrt{p}\mathbf{l}_{n1z}\mathbf{v}_{1z}} \times \begin{bmatrix} 0 & 0 & 0 & 0 & -\mathbf{v}_{1y}\sin\psi - \mathbf{v}_{1x}\cos\psi & \mathbf{v}_{1x}\sin\psi - \mathbf{v}_{1y}\cos\psi \\ 0 & \mathbf{v}_{1y}\sin\varphi - \mathbf{v}_{1x}\cos\varphi & \mathbf{v}_{1y}\cos\varphi + \mathbf{v}_{1x}\sin\varphi & 0 & 0 & 0 \\ 0 & 0 & 0 & \frac{\mathbf{v}_{1z}}{\sqrt{2}} & 0 & 0 \\ 0 & \mathbf{l}_{n1y}\cos\varphi + \mathbf{l}_{n1x}\sin\varphi & \mathbf{l}_{n1x}\cos\varphi - \mathbf{l}_{n1y}\sin\varphi & 0 & 0 & 0 \\ 0 & 0 & 0 & 0 & \mathbf{l}_{n1x}\sin\psi - \mathbf{l}_{n1y}\cos\psi & \mathbf{l}_{n1x}\cos\psi + \mathbf{l}_{n1y}sin\psi \\ \frac{\mathbf{l}_{n1z}}{\sqrt{2}} & 0 & 0 & 0 & 0 & 0 \end{bmatrix}, \quad (14)$$

https://doi.org/10.1017/S0263574714000526 Published online by Cambridge University Press

where

$$\cos\varphi = \frac{t_1}{\sqrt{t_1^2+1}},\ \sin\varphi = \frac{1}{\sqrt{t_1^2+1}}$$

$$t_1 = \frac{1}{2}\frac{\frac{m}{I_{xx}}\left(\mathbf{v}_{1x}^2-\mathbf{v}_{1y}^2\right)+\mathbf{l}_{n1y}^2-\mathbf{l}_{n1x}^2+\left(\left(\frac{m}{I_{xx}}\left(\mathbf{v}_{1y}^2-\mathbf{v}_{1x}^2\right)+\mathbf{l}_{n1x}^2-\mathbf{l}_{n1y}^2\right)^2+4\left(\frac{m}{I_{xx}}\mathbf{v}_{1y}\mathbf{v}_{1x}-\mathbf{l}_{n1x}\mathbf{l}_{n1y}\right)^2\right)^{\frac{1}{2}}}{-\frac{m}{I_{xx}}\mathbf{v}_{1y}\mathbf{v}_{1x}+\mathbf{l}_{n1x}\mathbf{l}_{n1y}}$$

$$\cos\psi = \frac{t_2}{\sqrt{t_2^2+1}},\ \sin\psi = \frac{1}{\sqrt{t_2^2+1}}$$

$$t_2 = \frac{1}{2}\frac{\frac{m}{I_{yy}}\left(\mathbf{v}_{1x}^2-\mathbf{v}_{1y}^2\right)+\mathbf{l}_{n1y}^2-\mathbf{l}_{n1x}^2+\left(\left(\frac{m}{I_{yy}}\left(\mathbf{v}_{1x}^2+\mathbf{v}_{1y}^2\right)+\mathbf{l}_{n1y}^2+\mathbf{l}_{n1x}^2\right)^2-4\frac{m}{I_{yy}}\left(\mathbf{l}_{n1x}\mathbf{v}_{1x}+\mathbf{l}_{n1y}\mathbf{v}_{1y}\right)^2\right)^{1/2}}{\frac{m}{I_{yy}}\mathbf{v}_{1y}\mathbf{v}_{1x}-\mathbf{l}_{n1x}\mathbf{l}_{n1y}}.$$

The modal matrix $\mathbf{U}$ is orthogonal with respect to either $\mathbf{M}_t$ or $\mathbf{K}_t$, which means $\mathbf{U}^{\mathrm{T}}\mathbf{M}_t\mathbf{U}=\mathbf{M}_d$ and $\mathbf{U}^{\mathrm{T}}\mathbf{K}_t\mathbf{U}=k\mathbf{E}_{6\times6}$, and $\mathbf{E}_{6\times6}$ is a six order identity matrix.

3.3. Coupling index of viscous damping

Using modal matrix $\mathbf{U}$, the modal damping matrix can be obtained:

$$\mathbf{D}=\mathbf{U}^{\mathrm{T}}\left(\mathbf{M}_t^{-1}\mathbf{B}_t\right)\mathbf{U}=\mathbf{M}_d^{-1}\left(\mathbf{U}^{\mathrm{T}}\mathbf{B}_t\mathbf{U}\right). \tag{15}$$

Combining Eqs. (11) and (13) gives Eq. (15) expressed as:

$$\mathbf{D}=\begin{bmatrix}\mathbf{\Lambda}_1 & \mathbf{0}_{3\times3}\\ \mathbf{0}_{3\times3} & \mathbf{\Lambda}_2\end{bmatrix}, \tag{16}$$

where

$$\mathbf{\Lambda}_1=\begin{bmatrix}D_{zz}&0&0\\0&D_{xxy}&\rho_{xxy}\\0&\rho_{yxx}&D_{yxx}\end{bmatrix},\quad \mathbf{\Lambda}_2=\begin{bmatrix}D_z&0&0\\0&D_{yyx}&\rho_{yyx}\\0&\rho_{xyy}&D_{xyy}\end{bmatrix}$$

$$D_{zz}=\lambda_1 B_{tzz}U_{61}^2,\ D_z=\lambda_4 B_{tz}U_{34}^2$$

$$D_{xxy}=\lambda_2\left(B_{ty}U_{22}^2+B_{txx}U_{42}^2+2\rho_{tz}U_{22}U_{42}\right),\quad D_{yxx}=\lambda_3\left(B_{ty}U_{23}^2+B_{txx}U_{43}^2+2\rho_{tz}U_{23}U_{43}\right)$$

$$D_{yyx}=\lambda_5\left(B_{tx}U_{15}^2+B_{tyy}U_{55}^2-2\rho_{tz}U_{15}U_{55}\right),\quad D_{xyy}=\lambda_6\left(B_{tx}U_{16}^2+B_{tyy}U_{56}^2-2\rho_{tz}U_{16}U_{56}\right)$$

$$\rho_{xxy}=\lambda_2\left(B_{ty}U_{22}U_{23}+B_{txx}U_{42}U_{43}+\rho_{tz}\left(U_{22}U_{43}+U_{23}U_{42}\right)\right)$$

$$\rho_{yxx}=\lambda_3\left(B_{ty}U_{22}U_{23}+B_{txx}U_{42}U_{43}+\rho_{tz}\left(U_{22}U_{43}+U_{23}U_{42}\right)\right)$$

$$\rho_{yyx}=\lambda_5\left(B_{tx}U_{15}U_{16}+B_{tyy}U_{55}U_{56}-\rho_{tz}\left(U_{15}U_{56}+U_{16}U_{55}\right)\right)$$

$$\rho_{xyy}=\lambda_6\left(B_{tx}U_{15}U_{16}+B_{tyy}U_{55}U_{56}-\rho_{tz}\left(U_{15}U_{56}+U_{16}U_{55}\right)\right)$$

Eq. (16) gives the coupling indices of the modal damping matrix $\mathbf{D}$, from which we can clearly distinguish the coupling effects in modal space. Note that the degrees of freedom (DOFs) of heave (z) and yaw (rz) are still decoupled, but the DOFs of surge (x) and pitch (ry), as well as sway (y) and roll (rx), which are fully decoupled when ignoring PJVF, are now coupled because of ρ_{xxy} and ρ_{yxx}, and ρ_{yyx} and ρ_{xyy}.

Define $D_\perp=|\rho_{xxy}|+|\rho_{yxx}|+|\rho_{yyx}|+|\rho_{xyy}|$ as coupling term and $D_o=D_{zz}+D_{xxy}+D_{yxx}+D_z+D_{yyx}+D_{xyy}$ as proportional damping term of the system and then the coupling term can be considered as perpendicular to the proportional damping term, seen in Fig. 2.

https://doi.org/10.1017/S0263574714000526 Published online by Cambridge University Press

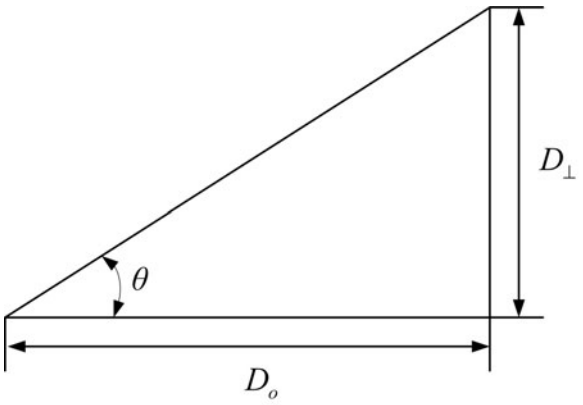

Fig. 2. The angle between coupling term $D_\perp$ and proportional damping term D_o.

According to the triangle theory and combining Eq. (4), the angle between coupling term and proportional damping term can be expressed as:

$$\theta = \arctan\left(\frac{D_\perp}{D_o}\right) = \arctan\left(\frac{|\rho_{xxy}| + |\rho_{yxx}| + |\rho_{yyx}| + |\rho_{xyy}|}{D_{zz} + D_{xxy} + D_{yxx} + D_z + D_{yyx} + D_{xyy}}\right), \tag{17}$$

where θ is an analytic formula for quantifying the coupling effects of viscous damping and $0^\circ \leq \theta < 90^\circ$. When $\theta = 0^\circ$ the system becomes a proportional damped system.

For ease of analysis, the index θ can be expressed as a function of the configuration parameters $(r_a, r_b, h, H, L, \alpha, \beta)$ and the payload inertial parameters $(m, I_{xx}, I_{yy}, I_{zz})$:

$$\mathbf{l}_{n,1} = \begin{bmatrix} \mathbf{l}_{n1x} & \mathbf{l}_{n1y} & \mathbf{l}_{n1z} \end{bmatrix}^{\mathrm{T}} = \begin{bmatrix} r_a\cos\alpha - r_b\cos\left(\frac{\pi}{p} - \beta\right) & r_a\sin\alpha - r_b\sin\left(\frac{\pi}{p} - \beta\right) & -H \end{bmatrix}^{\mathrm{T}}/L, \tag{18a}$$

where L denotes the strut length and $L = \sqrt{r_a^2 + r_b^2 - 2r_a r_b\cos(\frac{\pi}{p} - \alpha - \beta) + H^2}$.

$$\mathbf{a}_1 = \begin{bmatrix} \mathrm{a}_{1x} & \mathrm{a}_{1y} & \mathrm{a}_{1z} \end{bmatrix}^{\mathrm{T}} = [\, r_a\cos\alpha \quad -r_a\sin\alpha \quad h \,]^{\mathrm{T}}. \tag{18b}$$

Substituting Eq. (18) into Eq. (17) we obtain:

$$\theta = f(r_a, r_b, h, H, L, \alpha, \beta, m, I_{xx}, I_{yy}, I_{zz}). \tag{19}$$

Equation (19) means the configuration parameters are related to the degree of coupling caused by PJVF, which means we can redesign a system for minimizing the degree of coupling of viscous damping by changing the geometric design parameters.

4. The relationship between the degree of coupling caused by PJVF and the kinematic parameters

Defining radius ratio n:

$$n = \frac{r_a}{r_b}. \tag{20}$$

Then, the kinematic parameters become the five elements n, h, H, α, β, but it is still too complex to find the relationship between these elements and the degree of coupling caused by PJVF. For ease of analysis, we divided the kinematics parameters into two groups:

Case A: where H, α, β are fixed parameters and n, h are variable quantities.
Case B: where H, n, h are fixed parameters and α, β are variable quantities.

https://doi.org/10.1017/S0263574714000526 Published online by Cambridge University Press

Equation (19) then becomes a two-element optimizing problem:

$$\theta = f(n, h), \tag{21}$$

Or:

$$\theta = f(\alpha, \beta). \tag{22}$$

However, it is difficult to consider θ in a concise symbolic form at this stage. Next, we give a numerical example to demonstrate the relationship between these elements and the degree of coupling caused by PJVF.

We give the configuration parameters of the Delft SIMONA motion system (data adopted from the literature[19]) as follows (see Table I):

Table I. Configuration parameters.

Parameters	Descriptions	Values	Units
R_a	Distribution radius of upper joint points	1.60	m
R_b	Distribution radius of lower joint points	1.65	m
H	Platform height in neutral position	2.20	m
h	Height of payload mass center	−0.23	m
m	Payload mass	2600	kg
I_{XX}	Moment of inertia	2300	kg m^2
I_{YY}	Moment of inertia	2300	kg m^2
I_{ZZ}	Moment of inertia	3800	kg m^2
α	Half of the distributing angle for the upper joints	0.0625	rad
β	Half of the distributing angle for the lower joints	0.1828	rad

Note that $\mathbf{B}_t$ is a linear combination of five parts, including $\mathbf{B}_{cd1}, \mathbf{B}_{cd2}, \mathbf{B}_{cu1}, \mathbf{B}_{cu2}, \mathbf{B}_{cr}$, and the relationship between each part's influence on the coupling effects in modal space and on the kinematics parameters are depicted in Figs. 3 and 4.

We can clearly distinguish the degree of coupling effect caused by each part of PJVF which is the white point in Figs. 3 and 4. Note that each part of PJVF has different degrees of coupling for the same configuration parameters and the received optimal result is not a single point but an area which is blue in Figs. 3 and 4.

5. An Optimal Design Method

The index θ in analytical form allows us to scrutinize the relationship between configuration parameters and the degree of coupling caused by PJVF. We shall see that θ becomes a two-element optimizing problem by selecting proper restricted conditions. In this section, we present a novel optimal design method for minimizing the coupling effects of PJVF. First we discuss optimal conditions and then we list the optimal design procedures.

5.1. Optimal Conditions

According to the analysis of Section 4.1, when choosing n and h or α and β as optimal parameters, we can achieve minimized coupling effects for the PJVF. Thus, Eqs. (21) and (22) are taken as the functions for optimal design.

Considering each part of the PJVF, the normalized PJVF is expressed as:

$$\mathbf{B}_t = w_1\mathbf{C}_{cd1} + w_2\mathbf{C}_{cd2} + w_3\mathbf{C}_{cu1} + w_4\mathbf{C}_{cu2} + w_5\mathbf{C}_{cr}, \tag{23}$$

where w_1, w_2, w_3, w_4, w_5 are normalized weighting factors. Different weighting factors means different damping coefficients of each part of the PJVF

Note that although Eq. (23) is derived from the limb type of UCU (universal-cylindrical-universal), it still can be used for other limb types such as SPS (spherical-prismatic-spherical),

https://doi.org/10.1017/S0263574714000526 Published online by Cambridge University Press

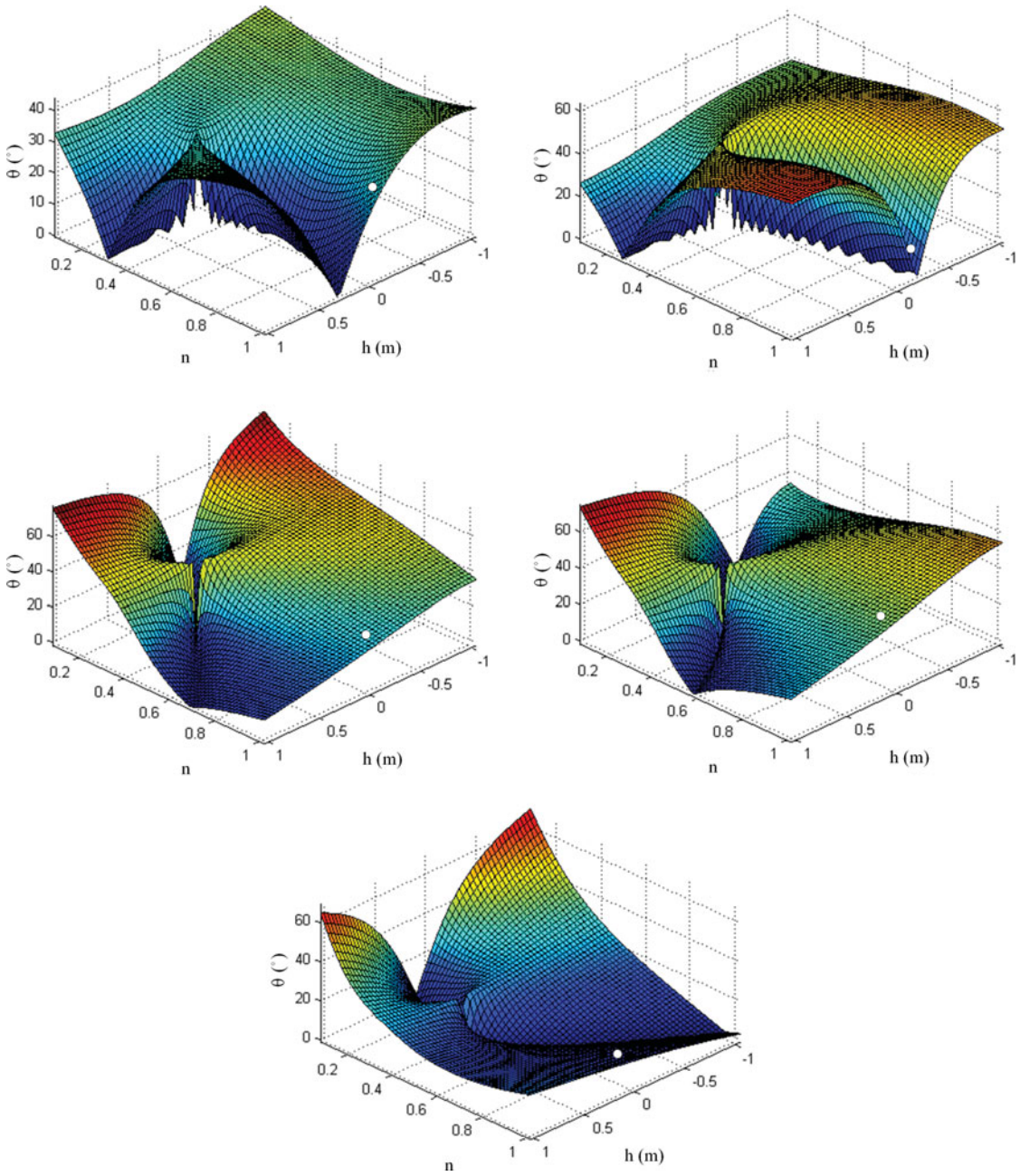

Fig. 3. The relationship between the degree of coupling caused by each part of PJVF and the parameters n, h.

UPS (universal-prismatic-spherical) or SPU(spherical-prismatic-universal) because

$$\mathbf{C}_{cd} = \sum_{i=1}^{2p} (\mathbf{J}_{di,x}^{\mathrm{T}} \mathbf{J}_{di,x}) = \mathbf{C}_{cd1} + \mathbf{C}_{cd2} \text{ and } \mathbf{C}_{cu} = \sum_{i=1}^{2p} (\mathbf{J}_{ui,x}^{\mathrm{T}} \mathbf{J}_{ui,x}) = \mathbf{C}_{cu1} + \mathbf{C}_{cu2}.$$

In other words, assuming $w_1 = w_2$, the damping matrix caused by the lower spherical joint can be expressed as $w_1\mathbf{C}_{\mathrm{cd1}} + w_2\mathbf{C}_{\mathrm{cd2}}$ and assuming $w_3 = w_4$, the damping matrix caused by the upper spherical joint can be expressed as $w_1\mathbf{C}_{cd1} + w_2\mathbf{C}_{cd2}$.

Two groups of optimization constraints were chosen in Section 4.1, but in practice, the strut length L may be used as an optimization constraint. With $L = \sqrt{r_a^2 + r_b^2 - 2r_a r_b \cos(\frac{\pi}{p} - \alpha - \beta) + H^2}$,

https://doi.org/10.1017/S0263574714000526 Published online by Cambridge University Press

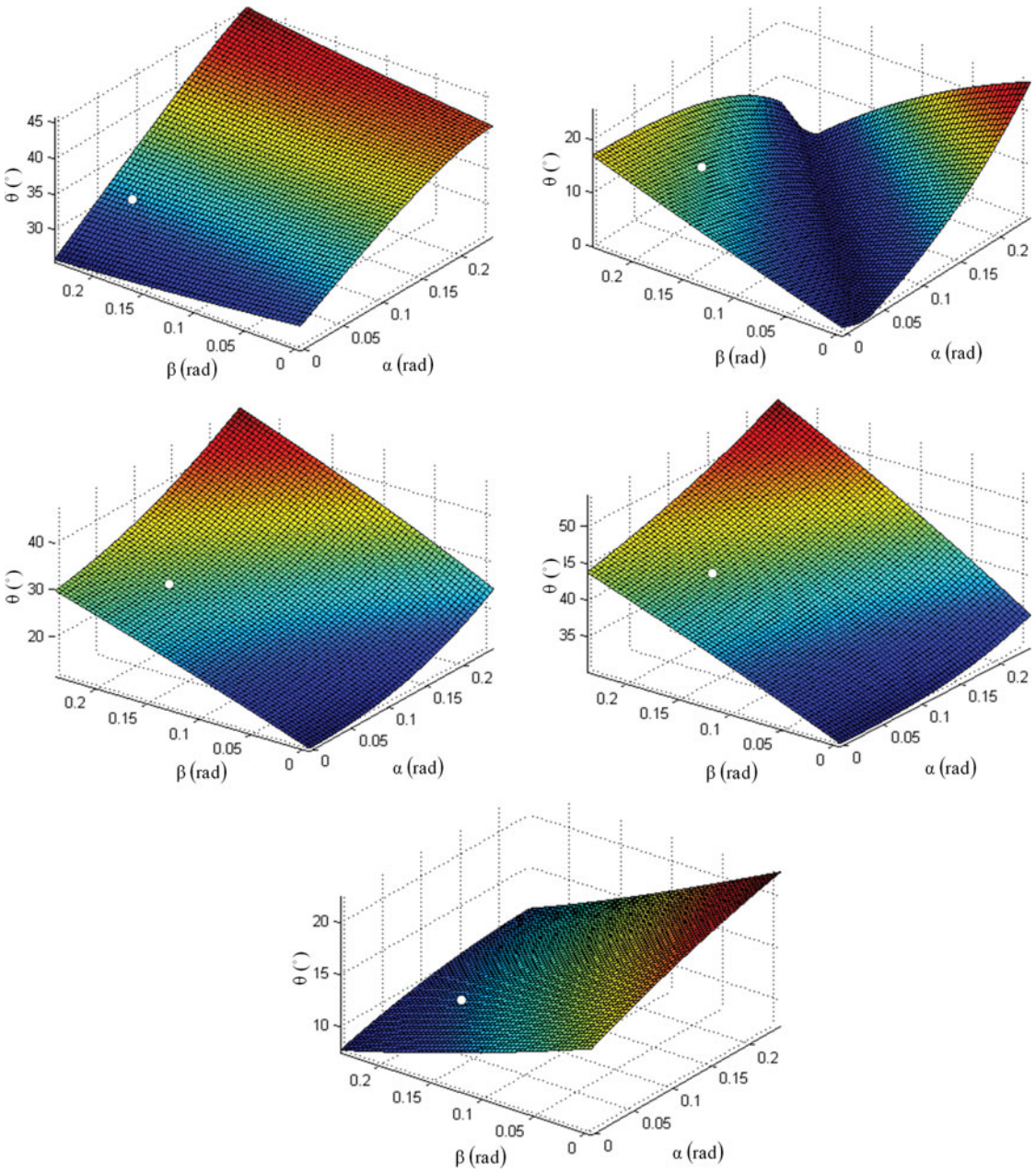

Fig. 4. The relationship between the degree of coupling caused by each part of PJVF and the parameters α, β.

another group of optimization constraints can still be used when the platform height in neutral position H is substituted by strut length L in Case A or Case B mentioned in Section 4.

5.2. Optimal design procedures

The above optimal conditions provide a solid foundation for a novel optimal design method for minimizing the coupling effects of PJVF. The iterative design procedures are listed as follows:

(a) Choose limb types (UCU, SPS, SPU, UPS) and Weighting Factors w_1, w_2, w_3, w_4, w_5.
(b) Choose optimization constraints

(Option a): $H, m, I_{xx}, I_{yy}, I_{zz}$
(Option b): $L, m, I_{xx}, I_{yy}, I_{zz}$

https://doi.org/10.1017/S0263574714000526 Published online by Cambridge University Press

Table II. Case A's Configuration parameters.

Parameters	Descriptions	Values	Units
R_a	Distribution radius of upper joint points	0.56	m
R_b	Distribution radius of lower joint points	1.20	m
L	Strut length	1.83	m
h	Height of payload mass center	−0.16	m
m	Payload mass	295.54	kg
I_{XX}	Moment of inertia	36.7075	kg m^2
I_{YY}	Moment of inertia	40.0476	kg m^2
I_{ZZ}	Moment of inertia	67.1330	kg m^2
α	half the distributing angle for the upper joints	0.2343	rad
β	half the distributing angle for the lower joints	0.1886	rad

Table III. Case B's Configuration parameters.

Parameters	Descriptions	Values	Units
R_a	Distribution radius of upper joint points	2.1148	m
R_b	Distribution radius of lower joint points	2.5170	m
L	Strut length	3.41	m
h	height of payload mass center	−1.772	m
m	Payload mass	13642	kg
I_{XX}	Moment of inertia	46477.1	kg m^2
I_{YY}	Moment of inertia	49396.1	kg m^2
I_{ZZ}	Moment of inertia	53865.0	kg m^2
α	Half the distributing angle for the upper joints	0.0541	rad
β	Half the distributing angle for the lower joints	0.0454	rad

(c) According to the optimal function Eq. (21), and assuming $\alpha = \beta = 0$, draw a 3D map which reflects the relationship between n, h, and θ, and find an acceptable optimal result n and h.
(d) According to the optimal function Eq. (22), draw a 3D map which reflects the relationship between α, β, and θ, and find an acceptable optimal result for α and β.
(e) Combining other technical specifications such as workspace volume, manipulability, dexterity, singularity, accuracy, actuator interference, and dynamic isotropy,[29] if some modifications are needed, return to step (b) and start another design iteration.

Next, we use an example to illustrate how to discover the architecture parameters based on the above design procedures. We obtained a Stewart–Gough platform (SGP) for the case $p = 3$, considered the influence of the payload inertial parameters, and used two configurations of SGP. Case A has small inertial parameters and Case B has larger inertial parameters, as shown in Tables II and III.

The redesign problem can now be described as: for each case, given the above inertial parameters of the payload, find a Stewart–Gough platform such that it is as close to a proportional damping system as possible. The limb type is UCU and the weighting factors are: $w_1 = w_2 = w_3 = w_4 = w_5 = 1$.

For Case A, we choose Option (b) which means the strut length is fixed. Using Eq. (20), we drew the 3D map depicted in Fig. 5.

The white circle point denotes the index θ. As can be deduced from Fig. 5, the index θ is 26.47°, and the kinematics parameters need to be optimized for decoupling in modal space.

When we choose $\theta \leq 10^\circ$ as an acceptable fault for modal space decoupling, the acceptable optimal result is the dark blue area in Fig. 5. The details of the result are discussed as follows:

For $n \leq 0.4$, the system is nonproportionally damped in most cases, although we can obtain an approximate proportionally damped system by changing the height h of the payload mass center, and the result is seriously sensitive.

For $0.4 < n \leq 0.8$, the system becomes proportionally damped when the center h of the payload mass is changed.

For $0.8 < n \leq 1$, the system can be considered proportionally damped.

https://doi.org/10.1017/S0263574714000526 Published online by Cambridge University Press

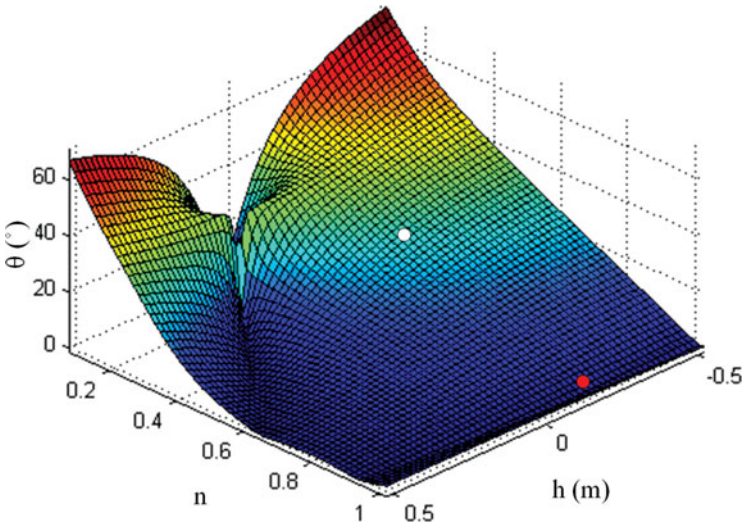

Fig. 5. The result of the optimized n and h for Case A.

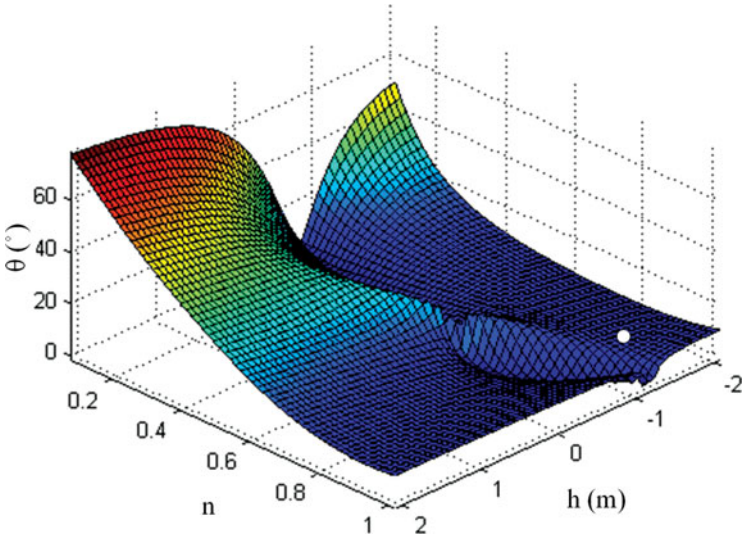

Fig. 6. The result of the optimized n and h for Case B.

When the center height h of the payload mass is fixed, the optimal radius ratio can be established as $n = 0.95$. The index θ is 1.40° which is the red point in Case A2 of Fig. 5.

For Case B, we choose Option (b) as optimization constraint. Using Eq. (21), we drew the 3D map depicted in Fig. 6.

As can be deduced from Fig. 6, the index θ is 7.29°, and the system can be considered as approximately proportionally damped in this case.

In contrast to Case A, the results for optimizing n and h are:

For $n \leq 0.4$, the system is nonproportionally damped.

For $0.4 < n \leq 0.8$, the system becomes proportionally damped with changes in the center h of the payload mass, where increasing or reducing the center h of the payload mass is a function of the inertial parameters.

For $0.8 < n \leq 1$, the system can be considered as proportionally damped.

For minimizing the degree of nonproportional damping further, using the optimal function, Eq. (22), we drew a 3D map which reflects the relationship between α, β, and θ as shown in Fig. 7.

The white point denotes the index θ for the two cases. For Case A, the index θ is 2.57°, and for case B, 5.38°. Optimizing α and β, we obtain a lower degree of coupling which is the red point. For Case A, the index θ is 0.092° when α is 0.2389 rad and β is 0.1401 rad, while for Case B, the index θ

https://doi.org/10.1017/S0263574714000526 Published online by Cambridge University Press

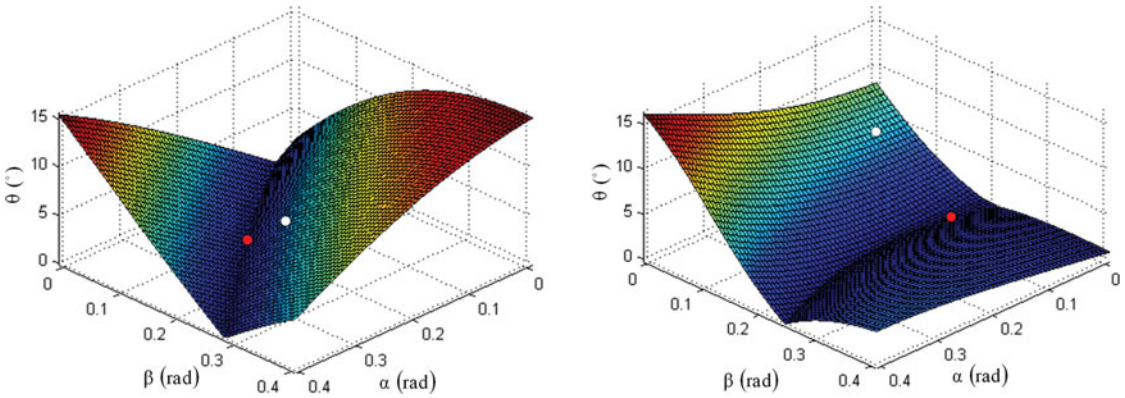

Fig. 7. The result for the optimized α and β.

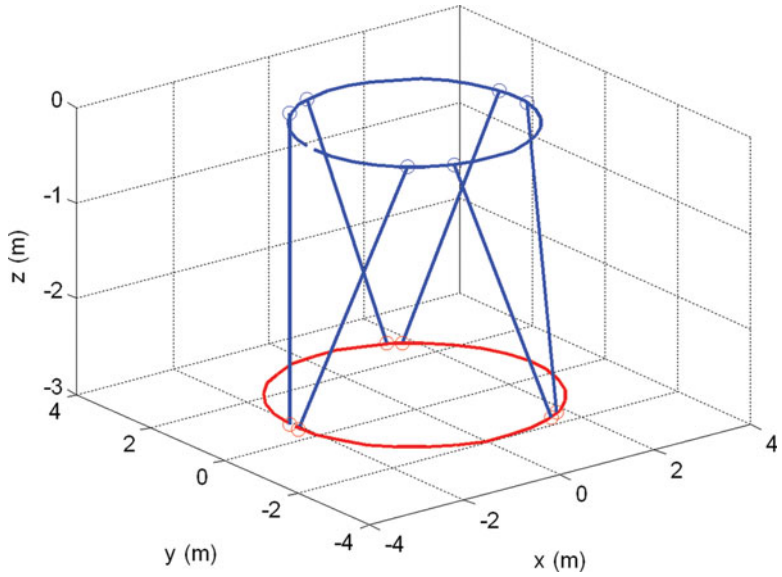

Fig. 8. Construction of modified SGP of Case B.

is 0.1952° when α is 0.05 rad and β is 0.1824 rad. Construction of modified SGP of Case B is shown in Fig. 8.

Although the above optimal design procedures assume the weighting factors are equal, the results still have enough tolerance provided by the result of the random combination of the five weighting factors w_1, w_2, w_3, w_4, w_5 as depicted in Fig. 9.

As can be deduced from Fig. 9, the index θ is lower than 15° in most cases, which can be considered a proportional damping system in engineering.

6. Conclusions

We presented an optimal design method for minimizing the coupling effects of PJVF for the SSPM.

Analytical formulation Jacobian matrixes relating the platform movements to each passive joint velocity were derived. With the formulation given, the damping matrix for PJVF was established.

Solving the undamped Eigen problem, an analytical formulation modal matrix was found and the index was then expressed as functions of the configuration parameters and the payload inertial parameters in analytical form.

From the above results, a two-element optimizing function was obtained. The relationship between the degree of coupling caused by each part of the PJVF and optimal parameters is explicit. It was found that an acceptable optimal result was not a single point but an area, and we can see that

https://doi.org/10.1017/S0263574714000526 Published online by Cambridge University Press

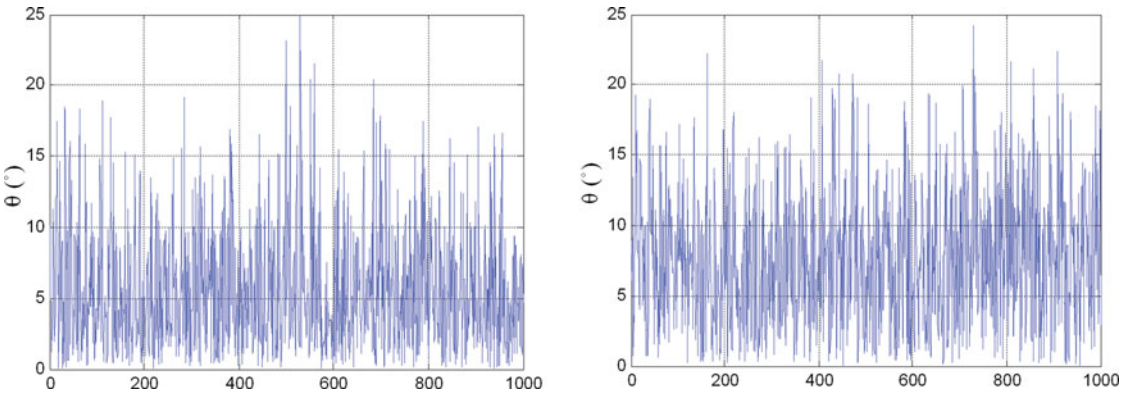

Fig. 9. The tolerance results.

it is possible to achieve an approximate proportionally damped system by adjusting the kinematic parameters.

Finally, we redesigned two cases for the SGP with different payload inertial parameters using the optimal design method proposed in this paper.

Acknowledgements

This work is financially supported by the National Natural Science Foundation of China (Grant No. 50975055 and No.51175100).

References

1. D. Stewart, "A platform with six degrees of freedom," *Proceedings of the IMechE* (UK) **180**(15), 371–385 (1965).
2. B. Dasgupta and T. S. Mruthyunjaya, "The Stewart Platform Manipulator: a Review," *Mech. Mach. Theory* **35**(1), 15–40 (2000).
3. J.-P. Merlet, *Parallel Robots* (Kluwer Academic Publishers, Netherlands, 2000).
4. J. E. McInroy and J. C. Hamann, "Design and control of flexure jointed hexapods," *IEEE Trans. Robot. Automat.*, **16**, 372–381 (Aug. 2000).
5. Y. Chen and J. E. McInroy, "Decoupled Control of Flexure-Jointed Hexapods using Estimated Joint-Space Mass-Inertia Matrix," *IEEE Transactions on Control Systems Technology* **12**(3), 413–421 (2004).
6. J. E. McInroy, J. F. O'Brien and A. Allais, "Designing dynamics and control of isotropic Gough-Stewart micromanipulators, Robotics and Automation (ICRA)," *2013 IEEE International Conference on*, Karlsruhe, Germany, (May 6–10, 2013) pp. 1458–1464.
7. A. R. Plummer and P. S. Guinzio, "Modal Control of an Electrohydrostatic Flight Simulator Motion System," *ASME 2009 Dynamic Systems and Control Conference*, Volume 2, Hollywood, California, USA (October 12–14, 2009).
8. A. R. Plummer, "Modal control for a class of multi-axis vibration table," *Control 2004*, Bath, UK (Sep. 2004).
9. A. R. Plummer, "Motion control for parallel overconstrained servohydraulic mechanisms," *The Tenth Scandinavian International Conference on Fluid Power, SICFP'07*, Tampere, Finland.
10. A. R. Plummer, "High bandwidth motion control for multiaxis servohydraulic mechanisms," *ASME International Mechanical Engineering Congress and Exposition*, Seattle, USA (Nov. 13–16, 2007) (Paper IMECE2007–41240).
11. K. A. Foss, "Co-ordinates which uncouple the equations of motion of damped linear dynamic systems," *ASME Journal of Applied Mechanics* **25**, 361–364 (1958).
12. A. S.Velestos and C. E.Ventura, "Modal analysis of non-classically damped linear systems," *Earthquake Engineering and Structural Dynamics* **14**, 217–243 (1986).
13. F. R. Vigneron, "An atural mode model and modal identities for damped linear dynamic structures," *ASME Journal of Applied Mechanics* **53**, 33–38 (1986).
14. K. Harib and K. Srinivasan, "Kinematic and dynamic analysis of Stewart platform-based machine tool structures," *Robotica* **21**(5), 541–554 (2003).
15. Reza Oftadeh, Mohammad M. Aref and D. Hamid, "Taghirad, Explicit Dynamics Formulation of Stewart–Gough Platform: A Newton–Euler Approach," *The 2010 IEEE/RSJ International Conference on Intelligent Robots and Systems*, Taipei, Taiwan (Oct. 18–22, 2010)

16. H. Abdellatif and B. Heimann, "Computational efficient inverse dynamics of 6-DOF fully parallel manipulators by using the Lagrangian formalism," *Mech. Mach. Theory* **44**, 192–207 (2009).
17. G. Lebret, K. Liu and F. L. Lewis, "Dynamic analysis and control of a Stewart platform manipulator," *J. Robot. Syst.* **10**(5), 629–655 (1993).
18. M. Liu, C. Li and C. Li, "Dynamics analysis of the Gough-Stewart platform manipulator," *IEEE Transactions on Robotics and Automation* **16**(1), 94–98 (2000).
19. S. H. Koekebakker, Model based control of a flight simulator motion system *PhD thesis* (Delft, Netherlands: Delft University of Technology, 2001).
20. D. L. Cronin, "Approximation for determining harmonically excited response of nonclassically damped systems," *ASME Journal of Engineering for Industry* **98**, 43–47 (1976).
21. K. R. Chung and C. W. Lee, "Dynamic reanalysis of weakly non-proportionally damped systems," *Journal of Sound and Vibration* **111**(1), 37–50 (1986).
22. S. M. Shahruz and F. Ma, "Approximate decoupling of the equations of motion of linear underdamped systems," *ASME Journal of Applied Mechanics* **55**, 716–720 (1988).
23. G. Prater and R. Singh, "Quantification of the extent of non-proportional viscous damping in discrete vibratory systems," *Journal of Sound and Vibration* **104**(1), 109–125 (1986).
24. J. Bellos and D. J. Inman, "Frequency response of nonproportionally damped, lumped parameter, linear dynamic systems," *ASME Journal of Vibration and Acoustics* **112**, 194–201 (1990).
25. M. Tong, Z. Liang and G. C. Lee, "An index of damping non-proportionality for discrete vibratory systems," *Journal of Sound and Vibration* **174**(1), 37–55 (1994).
26. K. Liu, M. R. Kujath and W. Zheng, "Evaluation of damping non-proportionality using identified modal information," *Mechanical Systems and Signal Processing* **15**(1), 227–242 (2001).
27. H. Z. Jiang, J. F. He and Z. Z. Tong, "Characteristics analysis of joint space inverse mass matrix for the optimal design of a 6-DOF parallel manipulator," *Mechanism and Machine Theory* **45**(5), 722–739 (2010).
28. J. F. He, H. Z. Jiang, Z. Z. Tong, B. P. Li and J. W. Han, "Study on dynamic isotropy of a class of symmetric spatial parallel mechanisms with actuation redundancy," *Journal of Vibration and Control* **18**(8), 1156–1164 (2012).
29. Z. Z. Tong, J. F. He, H. Z. Jiang and G. R. Duan, "Optimal design of a class of generalized symmetric Gough–Stewart parallel manipulators with dynamic isotropy and singularity-free workspace," *Robotica* **30**(2), 305–314 (2012).

Appendix A: Detailed kinematics analysis of passive joint

According to the relationship between the vector space, the length vectors of a $2p$ cylinder $\mathbf{l}_i$ ($i = 1, \ldots, 2p$) can be expressed as:

$$\mathbf{l}_i = \mathbf{c} + \mathbf{T}\mathbf{a}_i - \mathbf{b}_i, \tag{A1}$$

where $\mathbf{T}$ is the rotation matrix, $\mathbf{c}$ is the displacement vector of the center of $\{\mathrm{B}\}$ in $\{\mathrm{M}\}$, $\mathbf{a}_i$ is the vector of the upper joint in the fixed coordinates, $\mathbf{b}_i$ is the vector of the lower joint in the inertial coordinates.

Suppose $\mathbf{v}_{ai}$ is the velocity of the upper joints, which can be expressed as:

$$\mathbf{v}_{ai} = \dot{\mathbf{c}} + \boldsymbol{\omega} \times \mathbf{T}\mathbf{a}_i, \tag{A2}$$

where $\boldsymbol{\omega}$ is the angular velocity of $\{\mathrm{M}\}$ relative to $\{\mathrm{B}\}$ and $\dot{\mathbf{c}}$ is the velocity vectors of the center points of $\{\mathrm{M}\}$ in the $\{\mathrm{B}\}$.

Equation (A2) can also be expressed by the Jacobian transformation:

$$\mathbf{v}_{ai} = \begin{bmatrix} \mathbf{I} & \mathbf{T}\left(\tilde{\mathbf{A}}_i^m\right)^T \mathbf{T}^T \end{bmatrix} \dot{\mathbf{x}} = \mathbf{J}_{ai,x}\dot{\mathbf{x}}, \tag{A3}$$

where $\tilde{\mathbf{A}}_i^m$ is a skew symmetric matrix of the vector $\mathbf{a}_i$, $\dot{\mathbf{x}}$ is the platform velocity vector, and $\mathbf{J}_{ai,x}$ is the Jacobian matrix for the general velocity of the moving platform to the velocity of the upper attachment points.

The structure diagram of the actuator is shown in Fig. A1.

The angular velocity of the actuator can be expressed as:

$$\boldsymbol{\omega}_{ai} = \mathbf{l}_{n,i} \times \frac{\mathbf{v}_{ai}}{|\mathbf{l}_i|}, \tag{A4}$$

where $\mathbf{l}_{n,i}$ is the 3×1 unit vector of $\mathbf{l}_i$

https://doi.org/10.1017/S0263574714000526 Published online by Cambridge University Press

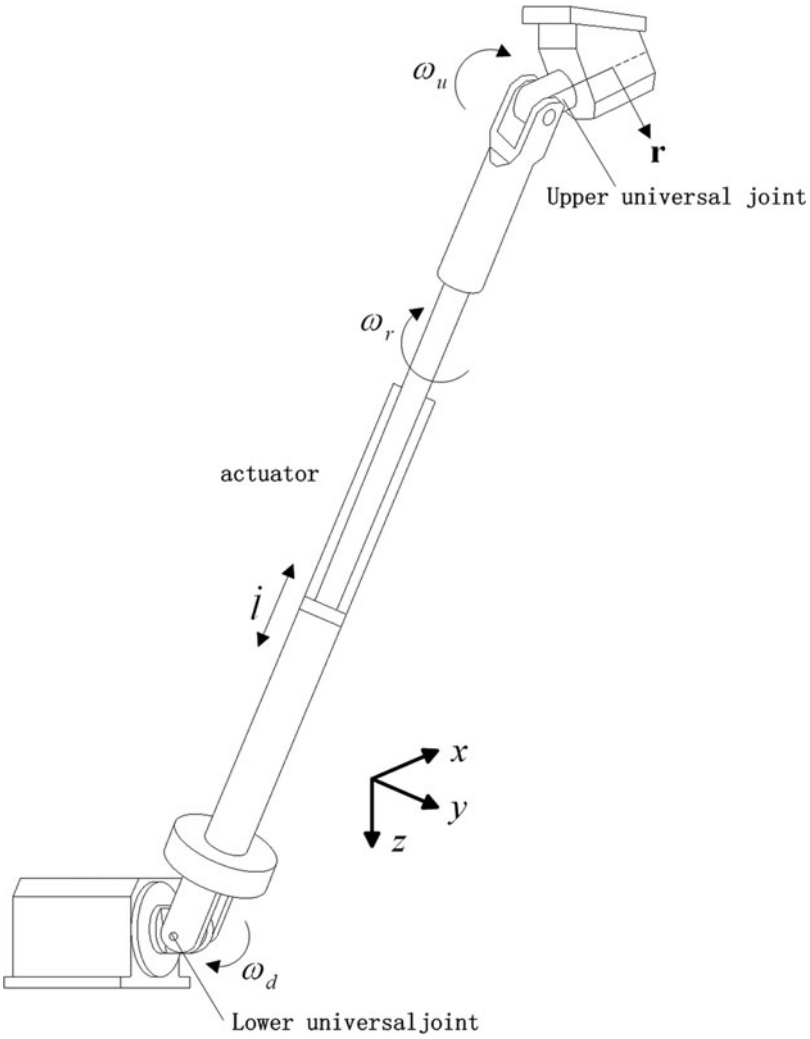

Fig. A1. SSPM actuator link construction.

The synthesis of the angular velocity of lower universal joint is expressed as:

$$\boldsymbol{\omega}_{d,i} = \boldsymbol{\omega}_{ai} = \left[\frac{\tilde{\mathbf{l}}_{n,i}}{|\mathbf{l}_i|} \quad \frac{1}{|\mathbf{l}_i|}\tilde{\mathbf{l}}_{n,i}\mathbf{T}\left(\tilde{\mathbf{A}}_i^m\right)^T \mathbf{T}^T \right] \dot{\mathbf{x}} = \mathbf{J}_{di,x}\dot{\mathbf{x}}, \tag{A5}$$

where $\tilde{\mathbf{l}}_{n,i}$ is a skew symmetric matrix of the vector $\mathbf{l}_{n,i}$

The directions of the lower universal joint axes are expressed as:

$$\begin{aligned} \mathbf{r}_{i,1} &= \mathbf{l}_{n,i} \times \mathbf{z} \\ \mathbf{r}_{ni,1} &= \frac{\mathbf{r}_{i,1}}{|\mathbf{r}_{i,1}|} \\ \mathbf{r}_{i,2} &= -\mathbf{r}_{ni,1} \times \mathbf{l}_{n,i} \\ \mathbf{r}_{ni,2} &= \frac{\mathbf{r}_{i,2}}{|\mathbf{r}_{i,2}|} \end{aligned}, \tag{A6}$$

where $\mathbf{z} = [0 \quad 0 \quad 1]^{\mathrm{T}}$

The decomposed angular velocity of lower universal joint is expressed as:

$$\begin{aligned} \boldsymbol{\omega}_{di,1} &= \left(\boldsymbol{\omega}_{d,i} \cdot \mathbf{r}_{ni,1}\right)\mathbf{r}_{ni,1} = \mathbf{r}_{ni,1}\left(\mathbf{r}_{ni,1} \cdot \boldsymbol{\omega}_{d,i}\right) = \mathbf{r}_{ni,1}\mathbf{r}_{ni,1}^{\mathrm{T}}\mathbf{J}_{di,x}\dot{\mathbf{x}} = \mathbf{J}_{di1,x}\dot{\mathbf{x}} \\ \boldsymbol{\omega}_{di,2} &= \left(\boldsymbol{\omega}_{d,i} \cdot \mathbf{r}_{ni,2}\right)\mathbf{r}_{ni,2} = \mathbf{r}_{ni,2}\left(\mathbf{r}_{ni,2} \cdot \boldsymbol{\omega}_{d,i}\right) = \mathbf{r}_{ni,2}\mathbf{r}_{ni,2}^{\mathrm{T}}\mathbf{J}_{di,x}\dot{\mathbf{x}} = \mathbf{J}_{di2,x}\dot{\mathbf{x}}. \end{aligned} \tag{A7}$$

https://doi.org/10.1017/S0263574714000526 Published online by Cambridge University Press

The synthesis of the angular velocity of upper universal joint is expressed as:

$$\boldsymbol{\omega}_{u,i} = \boldsymbol{\omega}_{d,i} + \boldsymbol{\omega}^m = \left[\frac{\tilde{\mathbf{l}}_{n,i}}{|\mathbf{l}_i|} \quad \frac{1}{|\mathbf{l}_i|}\tilde{\mathbf{l}}_{n,i}\mathbf{T}\left(\tilde{\mathbf{A}}_i^m\right)^T \mathbf{T}^T + \mathbf{T}^T \right] \dot{\mathbf{x}} = \mathbf{J}_{ui,x}\dot{\mathbf{x}}, \tag{A8}$$

where $\boldsymbol{\omega}^m$ is the angular velocity of $\{\mathrm{B}\}$ relative to $\{\mathrm{M}\}$.

The directions of the upper universal joint is expressed as:

$$\begin{aligned} \mathbf{r}_{i,3} &= \mathbf{l}_{n,i} \times \mathbf{Tr} \\ \mathbf{r}_{ni,3} &= \frac{\mathbf{r}_{i,3}}{|\mathbf{r}_{i,3}|} \\ \mathbf{r}_{i,4} &= -\mathbf{r}_{ni,3} \times \mathbf{l}_{n,i} \\ \mathbf{r}_{ni,4} &= \frac{\mathbf{r}_{i,4}}{|\mathbf{r}_{i,4}|} \end{aligned}, \tag{A9}$$

where $\mathbf{r}$ is the orthogonal axis with the installation plane of upper universal joint.

The decomposed angular velocity of upper universal joint is expressed as:

$$\begin{aligned} \boldsymbol{\omega}_{ui,1} &= \left(\boldsymbol{\omega}_{u,i} \cdot \mathbf{r}_{ni,3}\right)\mathbf{r}_{ni,3} = \mathbf{r}_{ni,3}\left(\mathbf{r}_{ni,3} \cdot \boldsymbol{\omega}_{u,i}\right) = \mathbf{r}_{ni,3}\mathbf{r}_{ni,3}^{\mathrm{T}}\mathbf{J}_{ui,x}\dot{\mathbf{x}} = \mathbf{J}_{ui1,x}\dot{\mathbf{x}} \\ \boldsymbol{\omega}_{ui,2} &= \left(\boldsymbol{\omega}_{u,i} \cdot \mathbf{r}_{ni,4}\right)\bar{\mathbf{r}}_{ni,4} = \mathbf{r}_{ni,4}\left(\mathbf{r}_{ni,4} \cdot \boldsymbol{\omega}_{u,i}\right) = \mathbf{r}_{ni,4}\mathbf{r}_{ni,4}^{\mathrm{T}}\mathbf{J}_{ui,x}\dot{\mathbf{x}} = \mathbf{J}_{ui2,x}\dot{\mathbf{x}} \end{aligned}, \tag{A10}$$

The revolute angular velocity of the actuator is expressed as:

$$\boldsymbol{\omega}_{r,i} = \left(\boldsymbol{\omega}^m \cdot \mathbf{l}_{n,i}\right)\mathbf{l}_{n,i} = \mathbf{l}_{n,i}\mathbf{l}_{n,i}^{\mathrm{T}}\left[\mathbf{0}_{3\times3} \quad \mathbf{T}^T\right]\dot{\mathbf{x}} = \mathbf{J}_{r,i}\dot{\mathbf{x}}. \tag{A11}$$

Appendix B: Derivation of $\mathbf{B}_t$

For ease of analysis, we assume the damping coefficients of each related passive joint are equal, which means $B_{cd1} = B_{cdi1}$, $B_{cd2} = B_{cdi2}$, $B_{cu1} = B_{cui1}$, $B_{cu2} = B_{cui2}$, $B_{cr} = B_{cri}$, with $i = 1, 2 \cdots 2p$.

The damping matrix for each related passive joint is expressed as

$$\mathbf{B}_{cd1} = B_{cd1}\mathbf{C}_{cd1} = B_{cd1}\begin{bmatrix} \mathrm{diag}([C_{cd1x} \quad C_{cd1y} \quad C_{cd1z}]^{\mathrm{T}}) & \tilde{\boldsymbol{\rho}}_{cd1} \\ -\tilde{\boldsymbol{\rho}}_{cd1} & \mathrm{diag}([C_{cd1xx} \quad C_{cd1yy} \quad C_{cd1zz}]^{\mathrm{T}}) \end{bmatrix}, \tag{B1}$$

where $\mathbf{B}_{cd1} = \sum_{i=1}^{2p}\left(B_{cd1}\mathbf{J}_{di1,x}^{\mathrm{T}}\mathbf{J}_{di1,x}\right)$ is the damping matrix in the direction of the lower universal joint axes $\mathbf{r}_{ni,1}$.

$$C_{cd1x} = C_{cd1y} = \frac{p}{|\mathbf{l}|^2}\mathbf{l}_{n1z}^2, \quad C_{cd1z} = \frac{2p}{|\mathbf{l}|^2}\left(1 - \mathbf{l}_{n1z}^2\right)$$

$$\mathrm{C}_{cd1xx} = \mathrm{C}_{cd1yy} = \frac{p}{|\mathbf{l}|^2}\left((\mathbf{l}_{n1x}\mathbf{a}_{1x} + \mathbf{l}_{n1z}\mathbf{a}_{1z})^2 + (\mathbf{l}_{n1y}\mathbf{a}_{1y} + \mathbf{l}_{n1z}\mathbf{a}_{1z})^2 + \left(\mathbf{l}_{n1x}^2\mathbf{a}_{1y}^2 + \mathbf{l}_{n1y}^2\mathbf{a}_{1z}^2 - \mathbf{l}_{n1z}^2\mathbf{a}_{1z}^2\right)\right)$$

$$\mathrm{C}_{cd1zz} = \frac{2p}{|\mathbf{l}|^2}\frac{\mathbf{l}_{n1z}^2}{1 - \mathbf{l}_{n1z}^2}\left(\mathbf{l}_{n1y}\mathbf{a}_{1x} - \mathbf{l}_{n1x}\mathbf{a}_{1y}\right)^2$$

$$\tilde{\boldsymbol{\rho}}_{cd1} = \begin{bmatrix} 0 & -\rho_{cd1z} & 0 \\ \rho_{cd1z} & 0 & 0 \\ 0 & 0 & 0 \end{bmatrix}, \quad \text{and} \quad \rho_{cd1z} = -\frac{p}{|\mathbf{l}|^2}\mathbf{l}_{n1z}\left(\mathbf{l}_{n1x}\mathbf{a}_{1x} + \mathbf{l}_{n1y}\mathbf{a}_{1y} + \mathbf{l}_{n1z}\mathbf{a}_{1z}\right)$$

$$\mathbf{B}_{cd2} = B_{cd2}\mathbf{C}_{cd2} = B_{cd2}\begin{bmatrix} \mathrm{diag}([C_{cd2x} \quad C_{cd2y} \quad 0]^{\mathrm{T}}) & \tilde{\boldsymbol{\rho}}_{cd2} \\ -\tilde{\boldsymbol{\rho}}_{cd2} & \mathrm{diag}([C_{cd2xx} \quad C_{cd2yy} \quad C_{cd2zz}]^{\mathrm{T}}) \end{bmatrix}, \tag{B2}$$

https://doi.org/10.1017/S0263574714000526 Published online by Cambridge University Press

where $\mathbf{B}_{cd2} = \sum_{i=1}^{2p} \left(B_{cdi2}\mathbf{J}_{di2,x}^{\mathrm{T}}\mathbf{J}_{di2,x}\right)$ is the damping matrix in the direction of the lower universal joint axes $\mathbf{r}_{ni,2}$.

$$
\begin{aligned}
&C_{cd2x} = C_{cd2y} = \frac{p}{|\mathbf{l}|^2}, \quad \mathrm{C}_{cd2xx} = \mathrm{C}_{cd2yy} = \frac{p}{|\mathbf{l}|^2}\mathbf{a}_{1z}^2 \\
&\mathrm{C}_{cd2zz} = \frac{2p}{|\mathbf{l}|^2}\frac{1}{1-\mathbf{l}_{n1z}^2}\left(\mathbf{l}_{n1x}\mathbf{a}_{1x} + \mathbf{l}_{n1y}\mathbf{a}_{1y}\right)^2 \\
&\tilde{\rho}_{cd2} = \begin{bmatrix} 0 & -\rho_{cd2z} & 0 \\ \rho_{cd2z} & 0 & 0 \\ 0 & 0 & 0 \end{bmatrix}, \quad \text{and} \quad \rho_{cd2z} = -\frac{p}{|\mathbf{l}|^2}\mathbf{a}_{1z} \\
&\mathbf{B}_{cu1} = B_{cu1}\mathbf{C}_{cu1} = B_{cu1}\begin{bmatrix} \mathrm{diag}([C_{cu1x} \quad C_{cu1y} \quad C_{cu1z}]^{\mathrm{T}}) & \tilde{\boldsymbol{\rho}}_{cu1} \\ -\tilde{\boldsymbol{\rho}}_{cu1} & \mathrm{diag}([C_{cu1xx} \quad C_{cu1yy} \quad C_{cu1zz}]^{\mathrm{T}}) \end{bmatrix},
\end{aligned}
\tag{B3}
$$

where $\mathbf{B}_{cu1} = \sum_{i=1}^{2p} \left(B_{cui1}\mathbf{J}_{ui1,x}^{\mathrm{T}}\mathbf{J}_{ui1,x}\right)$ is the damping matrix in the direction of the upper universal joint axes $\mathbf{r}_{ni,3}$.

$$
\begin{aligned}
&C_{cu1x} = C_{cu1y} = \frac{p}{|\mathbf{l}|^2}\mathbf{l}_{n1z}^2, \quad C_{cu1z} = \frac{2p}{|\mathbf{l}|^2}\left(1-\mathbf{l}_{n1z}^2\right) \\
&\mathrm{C}_{cu1xx} = \mathrm{C}_{cu1yy} = \frac{p}{|\mathbf{l}|^2}\left(\begin{array}{c} |\mathbf{l}|^2 - 2\,|\mathbf{l}|\,(\mathbf{l}_{n1x}\mathbf{a}_{1x} + \mathbf{l}_{n1y}\mathbf{a}_{1y} + \mathbf{l}_{n1z}\mathbf{a}_{1z}) + (\mathbf{l}_{n1x}\mathbf{a}_{1x} + \mathbf{l}_{n1z}\mathbf{a}_{1z})^2 \\ +(\mathbf{l}_{n1y}\mathbf{a}_{1y} + \mathbf{l}_{n1z}\mathbf{a}_{1z})^2 + \left(\mathbf{l}_{n1x}^2\mathbf{a}_{1y}^2 + \mathbf{l}_{n1y}^2\mathbf{a}_{x}^2 - \mathbf{l}_{n1z}^2\mathbf{a}_{1z}^2\right) \end{array}\right) \\
&\mathrm{C}_{cu1zz} = \frac{2p}{|\mathbf{l}|^2}\frac{\mathbf{l}_{n1z}^2}{1-\mathbf{l}_{n1z}^2}\left(\mathbf{l}_{n1y}\mathbf{a}_{1x} - \mathbf{l}_{n1x}\mathbf{a}_{1y}\right)^2 \\
&\tilde{\boldsymbol{\rho}}_{cu1} = \begin{bmatrix} 0 & -\rho_{cu1z} & 0 \\ \rho_{cu1z} & 0 & 0 \\ 0 & 0 & 0 \end{bmatrix}, \quad \text{and} \quad \rho_{cu1z} = -\frac{p}{|\mathbf{l}|^2}\mathbf{l}_{n1z}\left(|\mathbf{l}| - \left(\mathbf{l}_{n1x}\mathbf{a}_{1x} + \mathbf{l}_{n1y}\mathbf{a}_{1y} + \mathbf{l}_{n1z}\mathbf{a}_{1z}\right)\right) \\
&\mathbf{B}_{cu2} = B_{cu2}\mathbf{C}_{cu2} = B_{cu2}\begin{bmatrix} \mathrm{diag}([C_{cu2x} \quad C_{cu2y} \quad 0]^{\mathrm{T}}) & \tilde{\boldsymbol{\rho}}_{cu2} \\ -\tilde{\boldsymbol{\rho}}_{cu2} & \mathrm{diag}([C_{cu2xx} \quad C_{cu2yy} \quad C_{cu2zz}]^{\mathrm{T}}) \end{bmatrix},
\end{aligned}
\tag{B4}
$$

where $\mathbf{B}_{cu2} = \sum_{i=1}^{2p} \left(B_{cui2}\mathbf{J}_{ui2,x}^{\mathrm{T}}\mathbf{J}_{ui2,x}\right)$ is the damping matrix in the direction of the upper universal joint axes $\mathbf{r}_{ni,4}$.

$$
\begin{aligned}
&C_{cu2x} = C_{cu2y} = \frac{p}{|\mathbf{l}|^2}, \quad C_{cu2xx} = C_{cu2yy} = \frac{p}{|\mathbf{l}|^2}\left(\mathbf{a}_{1z} - |\mathbf{l}|\,\mathbf{l}_{n1z}\right)^2 \\
&\mathrm{C}_{cu2zz} = \frac{2p}{|\mathbf{l}|^2}\frac{1}{1-\mathbf{l}_{n1z}^2}\left(\left(\mathbf{l}_{n1x}\mathbf{a}_{1x} + \mathbf{l}_{n1y}\mathbf{a}_{1y}\right) - |\mathbf{l}|\left(1-\mathbf{l}_{n1z}^2\right)\right)^2 \\
&\tilde{\boldsymbol{\rho}}_{cu2} = \begin{bmatrix} 0 & -\rho_{cu2z} & 0 \\ \rho_{cu2z} & 0 & 0 \\ 0 & 0 & 0 \end{bmatrix}, \quad \text{and} \quad \rho_{cu2z} = -\frac{p}{|\mathbf{l}|^2}\left(\mathbf{a}_{1z} - |\mathbf{l}|\,\mathbf{l}_{n1z}\right) \\
&\mathbf{B}_{cr} = B_{cr}\mathbf{C}_{cr} = B_{cr}\begin{bmatrix} \bar{\mathbf{0}}_{3\times3} & \bar{\mathbf{0}}_{3\times3} \\ \bar{\mathbf{0}}_{3\times3} & \mathrm{diag}([C_{crxx} \quad C_{cryy} \quad C_{crzz}]^{\mathrm{T}}) \end{bmatrix},
\end{aligned}
\tag{B5}
$$

https://doi.org/10.1017/S0263574714000526 Published online by Cambridge University Press

where $\mathbf{B}_{cr} = \sum_{i=1}^{2p} \left(B_{cri}\mathbf{J}_{r,i}^{\mathrm{T}}\mathbf{J}_{r,i}\right)$ is the damping matrix in the revolute direction of the actuator.

$$C_{crxx} = C_{cryy} = p\left(1 - \mathbf{l}_{n1z}^2\right), \quad C_{crzz} = 2p\mathbf{l}_{n1z}^2.$$

Combining Eqs. (B1–B5), $\mathbf{B}_t$ is expressed as

$$\mathbf{B}_t = \begin{bmatrix} \mathrm{diag}([B_{tx} \quad B_{ty} \quad B_{tz}]^{\mathrm{T}}) & \tilde{\boldsymbol{\rho}}_t \\ -\tilde{\boldsymbol{\rho}}_t & \mathrm{diag}([B_{txx} \quad B_{tyy} \quad B_{tzz}]^{\mathrm{T}}) \end{bmatrix}, \tag{B6}$$

where:

$$\begin{aligned}
B_{tx} &= B_{cd1}C_{cd1x} + B_{cd2}C_{cd2x} + B_{cu1}C_{cu1x} + B_{cu2}C_{cu2x} \\
B_{ty} &= B_{cd1}C_{cd1y} + B_{cd2}C_{cd2y} + B_{cu1}C_{cu1y} + B_{cu2}C_{cu2y} \\
B_{tz} &= B_{cd1}C_{cd1z} + B_{cd2}C_{cd2z} \\
B_{txx} &= B_{cd1}C_{cd1xx} + B_{cd2}C_{cd2xx} + B_{cu1}C_{cu1xx} + B_{cu2}C_{cu2xx} + B_{cr}C_{crxx} \\
B_{tyy} &= B_{cd1}C_{cd1yy} + B_{cd2}C_{cd2yy} + B_{cu1}C_{cu1yy} + B_{cu2}C_{cu2yy} + B_{cr}C_{cryy} \\
B_{tzz} &= B_{cd1}C_{cd1zz} + B_{cd2}C_{cd2zz} + B_{cu1}C_{cu1zz} + B_{cu2}C_{cu2zz} + B_{cr}C_{crzz} \\
\tilde{\boldsymbol{\rho}}_t &= \begin{bmatrix} 0 & -\rho_{tz} & 0 \\ \rho_{tz} & 0 & 0 \\ 0 & 0 & 0 \end{bmatrix}, \quad \text{and} \quad \rho_{tz} = B_{cd1}\rho_{cd1z} + B_{cd2}\rho_{cd2z} + B_{cu1}\rho_{cu1z} + B_{cu2}\rho_{cu2z}
\end{aligned}$$

https://doi.org/10.1017/S0263574714000526 Published online by Cambridge University Press